Progress In Electromagnetics Research C, Vol. 135, 1–11, 2023

Analysis and Fabrication of Conductive Strip and Paint-Based Hemispherical Helical Antennas on 3D Printed Structure

Purno Ghosh* **and Frances J. Harackiewicz**

Abstract—Fabrication of a non-planar helical antenna while maintaining mechanical stability and durability is always challenging. Moreover, impedance matching is an issue for helix-type antennas. To ease the fabrication challenge, the advantage of additive manufacturing is utilized. For achieving self-matching, radiating spiral conductors in the forms of a strip and thick wire are used as two independent techniques. Consequently, a 3-turn hemispherical helical antenna (HHA) is analyzed by varying the width of the strip and the diameter of the wire. The better-performing HHA is again investigated including the effect of Poly-lactic acid (PLA) material-based supportive structure. At the initial step of fabrication, a 3-D printer is used to have the complete support structure. For ensuring the metallic part, copper strips and conductive paints are used as two different approaches. The measured data validates that both strip and wire-based HHA are self-matched. Circular polarization is obtained over wide frequency bands with axial ratio bandwidth (AR BW) of 35%. The maximum gain and beamwidths under 3-dB AR BW are 9.35 dBi and 118°, respectively. The mechanically stable, low profile, and wideband circular polarization favored the use of HHA in satellite communication.

1. INTRODUCTION

Depending on the applications, various types of antennas can produce circular polarizations [1, 2]. Besides this, individual antennae can be used as a part of the array elements for multiple-input multiple-output (MIMO) applications where a fractal-based geometry is very common [3–6]. Helical antennas are also a good candidate to produce circular polarization. Traditional cylindrical helix is an example that provides circular polarization in an axial direction, but the physical size and low beamwidths are two major limitations. To maintain the low profile along with wide angular range, several studies on hemispherical helical antennae have already been performed, where conductive wire and tapered metallic strips were mainly used as radiating parts. The study on a complete spherical helical antenna was performed in [7], where circular polarization with wide beamwidth was achieved, but due to the use of a full sphere, the physical size and stability issues were a matter of concern, and no construction was reported. A balanced ball fully spherical shape antenna in dipole form was presented in [8] which used polymethacrylimide foam as support. It required making a track or carving manually onto the surface of the foam for placing the conductive wire. A wire-based low-profile hemispherical antenna with a wire radius of 0.5 mm was studied in [9], but the fabrication process and prototype structure were not shown. Furthermore, the antenna did not provide an input impedance comparable to the traditional transmission line impedance of 50 Ω. Two layers of dielectric materials were used in [10] as supportive parts as well as an improvement of % 3 dB AR BW for wire-based HHA where the wire radius was 0.5 mm. After adding one more dielectric layer, 5% 3 dB AR BW and 100° of beamwidth were found, and the impedance matching was accomplished by extra wire segments. A wire-based hemispherical antenna has been discussed in [11], but an extra conductive strip inside the hemispherical volume was

Received 2 May 2023, Accepted 21 June 2023, Scheduled 14 July 2023
* Corresponding author: Purno Ghosh (purno.ghosh@siu.edu).
The authors are with the Southern Illinois University, USA.

used for impedance matching. It was claimed that the copper wire of the antenna was wrapped in foam, but no prototype of the fabricated structure was shown. Another wire-formed 3D-printed hemispherical antenna has been demonstrated in [12] where feeding was established at the pole of the hemisphere. Two different dielectric materials namely PETG and ABS were used there for support and circular dielectric wire. Since the dielectric wire was 3D printed on the support, there was a chance of missing the electroless plating on the back side of the wire. Moreover, there was no indication of the diameter or surface area of the conductive part. Instead of circular conductive wire, tapered metallic strip-based HHA was analyzed in [13] where an extra section of the strip was used for the impedance matching, and balsa wood was used as the support structure. A numerical study on HHA with two flake-like arms for improved performances has been reported in [14] which required wideband balun and extra absorbing material. A strip-based hemispherical helical antenna was analyzed in [15] where impedance matching was achieved by adding three extra small parts of strips, and polystyrene foam was used for support. For rapid prototyping of an electrically small hemispherical antenna, conductive paint was used on the 3D-printed dielectric wire [16]. Strip-based low-profile cylindrical and semi-ellipsoidal helical antennas have been successfully fabricated on the 3D-printed support structure [17, 18]. Beyond hemispherical shape, strip-based conical and cylindrical helix antennas irrespective of strip orientation have been analyzed in [19–22], but none of the work reported a rapid and stable construction method. The review article [23] showed the successful use of additive manufacturing in the fabrication of different types of antennae except for strip and thick wire-based 3D spiral antennas. Although a few works are done on strip-based HHA, impedance matching and reliable prototyping were always a concern. It is evident that all the above-reported works on hemispherical helical antennae either required an extra impedance matching section for impedance matching or required a stable support structure for reliable fabrication.

In this work, along with solving fabrication complexities and impedance matching issues, analysis was also done rigorously by varying the widths of the strip and the diameter of the wire. Non-conformal placement of the strip conductor relative to the hemispherical surface facilitates self-matching of impedance. On the other hand, wire with a wider diameter solved the impedance matching issue. Since 3-D printing provides design and construction flexibilities, conductive elements of any shapes and orientations can be implemented on a suitable support structure which was efficiently done in this work.

2. GEOMETRY AND DESIGN OF STRIP-BASED HHA

Due to the use of only half of the spherical area, the hemispherical helical antenna is smaller in size and considered a low profile. The size of the HHA does not change with a varying number of turns which makes it advantageous to control antenna performance parameters in fixed antenna size. The geometry of the wire-based HHA is shown in Fig. 1(a) where the spacing between adjacent turns is constant.

As already shown in [13], the hemispherical geometry maintains the following relations in the spherical coordinate system: $r = a$, and $\theta = \cos^{-1}(\varphi/N\pi)$ with $0 \leq \varphi \leq N\pi$. The hemispherical radius is indicated as 'a', and 'N' is the number of hemispherical turns. The design of a strip-based HHA started from the design of wire-based configuration, and the radius of the outer edge of the strip is the same as the radius of the hemisphere. Both wire and strip-based designs were performed in CST Microwave Studio, and the analytical 'curve' and 'face' options were used to create a circular wire and spiral face, respectively. To do so, the following parametric equations were developed in CST:

$$X(u) = a\sin(u)\cos(4Nu) \tag{1}$$

$$Y(u) = a\sin(u)\sin(4Nu) \tag{2}$$

$$Z(u,v) = a\cos(u) + v \tag{3}$$

where $u = 0$ to $\pi/2$ and $v = 0$ to t, where t is the thickness of the strip.

Then, the created face is widened toward the center of the hemisphere by using the option of 'thicken sheet' and a parameter 'W' set to control the width of the strip. The strip-based hemispherical antenna is shown in Fig. 1(b). In this design, the radius (a) of the hemisphere is considered 23 mm. The wire radius and strip widths are varied, and the details are discussed in Section 3.1. Analysis is carried out by considering the number of spiral turns 3, and the HHA is oriented along the XY plane. The gap (h) between the feed end and the ground plane is 3 mm, and the optimized side (S) of the square ground plane is 100 mm.

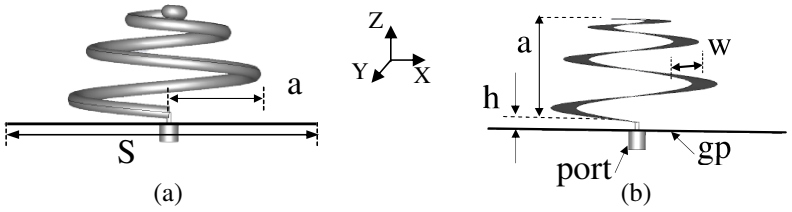

Figure 1. Geometry of HHA. (a) Wire-based, (b) strip-based.

3. SIMULATION RESULTS

The simulation analysis is divided into two parts. In one part, strip and wire-based HHA are analyzed by varying the width of the strip and the diameter of the wire. In the other part, better performing HHA is investigated along with the supportive structure.

3.1. Numerical Analysis for Conductive Parts Only

For the HHA, radiating conductors are used in two different forms namely flat strips of constant width and wire of circular cross-section. To observe the performance matrices of the antenna, the widths of the strip and wire radius are varied. So, for a fixed number of turns ($N = 3$), strip widths (W) are varied from 5 mm to 9 mm with an interval of 2 mm. It is seen from Fig. 2 that impedance can be matched ($S_{11} \leq -10$ dB) without any extra matching section when the strip width (W) is above 3 mm. In [13], the numerical analysis was limited to constant strip width ($W = 2$ mm), the number of turns ($N = 4.5$), and the maximum width of 4 mm for the case of tapered strip arm, where an extra matching section was used. For circular thin wire, impedance matching was always an issue that was discussed in the reported work in the introduction section. But using a thicker wire (wide cross-section), the issue can be solved. In this work, the radius of the wire is varied from 1.5 mm to 3 mm. Although it is seen from Fig. 2 that for any of the considered radii, the antenna is self-matched, but an additional matching section is required when the radius is below 1 mm which is not shown in this figure. To observe the impedance matching beyond the operational frequency, analysis is carried out to the extended frequency of 10 GHz. It is observed that ultrawideband impedance matching can be obtained when the strip width is wide, and placement is non-conformal relative to the hemispherical surface. The hemispherical helical antenna produces circular polarization which is one of the important performance parameters and can be represented in terms of axial ratio (AR). The 3-dB AR BW increases up to a certain strip width (W) of 7 mm which is shown in Fig. 3. A strip width of $W = 7$ mm provides the maximum 3-dB AR BW of 35.2% (2.81 GHz to 4.01 GHz). Wire diameter also has an impact on AR values as well as on circular polarization. It is seen from Fig. 3 that a maximum of 29.43% (2.55 GHz to 3.43 GHz) 3-dB AR BW is achieved for the median wire radius of 2.25 mm. For the wire-based case, the lower frequency

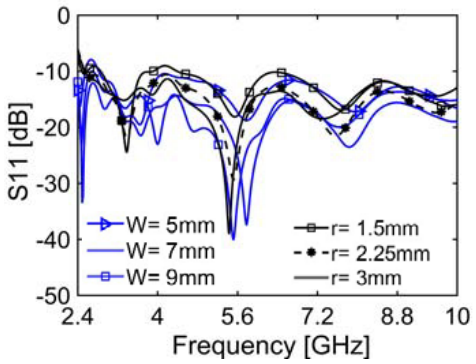

Figure 2. Impacts of strip widths (W) and wire radius (r) on reflection coefficient.

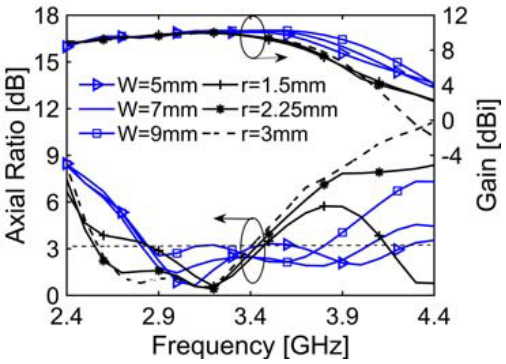

Figure 3. Impacts of strip widths (W) and wire radius (r) on axial ratio and gain.

in the covered AR BW started earlier than the strip-based case, and it is because of the decreasing gap between turns due to the increase of wire radius. For both strip and wire-based cases, gain almost follows the same pattern irrespective of the width of the strip and the radius of the wire. Under the covered AR BW range, there is a small variation of gain among various strip widths as shown in Fig. 3. For $W = 7\,\text{mm}$ and $r = 2.25\,\text{mm}$, gain variations under $AR \leq 3\,\text{dB}$ are $9 \pm 1.4\,\text{dBi}$ and $9.45 \pm 0.55\,\text{dBi}$, respectively.

For various strip widths and wire radii, beamwidths are also observed at 3 GHz in the XZ plane and are shown in Fig. 4. It is seen that beamwidth increases with increasing strip width, and based on the overall AR purity (AR values toward 0 dB), $W = 7\,\text{mm}$ provides 3-dB AR beamwidth of 93°. Similarly, for the wire-based case, a maximum 3-dB AR beamwidth of 98° is observed. Depending on the above performances of 3-dB AR BW, gain, and beamwidth, 3-turns HHA with a strip width of 7 mm and wire radius of 2.25 mm is chosen for further analysis including a PLA material-based supportive structure. It is needed to mention that for the wire-based case, the circular wire is made hollow from solid, and due to this change, no significant variation is observed regarding performance parameters.

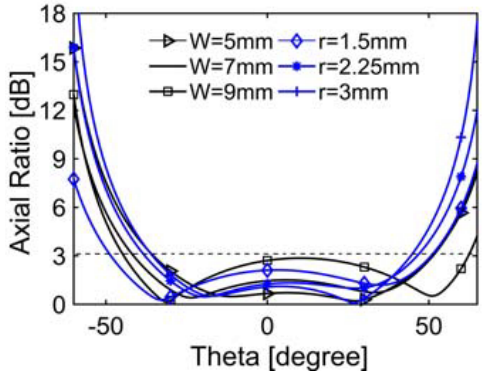

Figure 4. Impacts of strip widths (W) and wire radius (r) on 3-dB AR beamwidths.

3.2. Numerical Analysis Including the Supportive Structure

In this step, tree-like supportive structures are also designed using CST. This extra support later eases the construction difficulties and improved mechanical stability. The complete supportive structure including associated dimensions is shown in Fig. 5. For both (strip and wire) cases, this extra supportive structure consists of a square base (side, S) for making the ground plane and a central round pillar (diameter, d_1) along with branches (diameter, d_2). These branches help to hold the flat spiral arm of width (W) and round wire of radius (r). The dielectric constant and loss tangent of the supportive material are considered as 3.11 and 0.013, respectively.

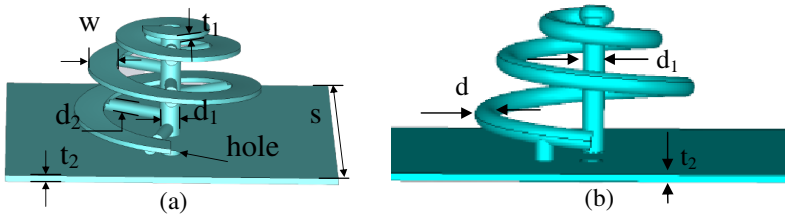

Figure 5. HHA with support structure: (a) Strip-based, (b) Thick wire-based. $W = 7\,\text{mm}$, $d_1 = 4\,\text{mm}$, $d_2 = 2.5\,\text{mm}$, $d = 2.25\,\text{mm}$, $t_1 = 1.5\,\text{mm}$, $t_2 = 2\,\text{mm}$, $S = 100\,\text{mm}$.

After simulating the HHA along with a supportive structure, it is observed that the reflection coefficient (S_{11}) values are very consistent with the wire-only case, and $S_{11} \leq -10\,\text{dB}$ is maintained through the considered maximum frequency (10 GHz) and shown in Fig. 6. Although there is a

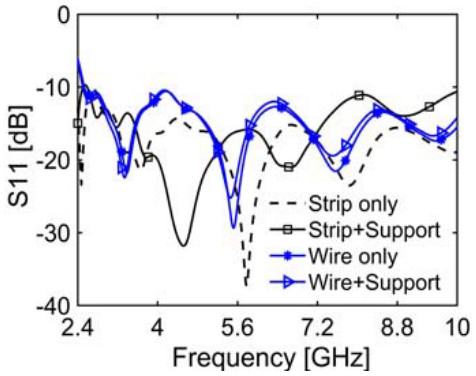

Figure 6. Impacts of support structure on S_{11}.

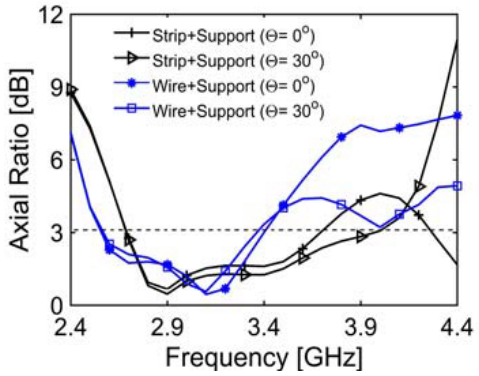

Figure 7. Impacts of support structure on axial ratio at boresight and further away.

discrepancy in the S_{11} pattern between strip and strip-with-support, it still maintains $S_{11} \leq -10\,\text{dB}$. The axial ratio bandwidth is analyzed at two different elevation angles namely $\theta = 0°$ and 30°. It is seen from Fig. 7 that due to the support, the lower frequency in the AR BW range starts earlier (compared with $W = 7\,\text{mm}$ in Fig. 3), and a 3-dB AR BW of 31.61% (2.69 GHz to 3.70 GHz) is achieved. In this case, wide dielectric support for the spiral arm increases the electrical length and width of the strip conductor. This increase of the width further increases the diameter of the hemisphere, resulting in the early start of lower frequency. Due to this impact, the overall percentage of 3-dB AR BW from the strip-only case is decreased. Bandwidth is also increased from the boresight ($\theta = 30°$). For the wire-based case, the impact of support structure on AR BW is very negligible, and the obtained percentage AR BW is 29.05% (2.56 GHz to 3.43 GHz) which is smaller than the strip-based case. In this case, bandwidth is almost constant at two different elevation angles. Gain values among all cases (strip, wire, and with their supports) are very consistent up to 3.3 GHz, and then start to decrease. No significant gain variation is observed between wire and wire-with-support, but there is a degradation for the cases of strip and strip-with-support which is shown in Fig. 8. This decrease in the gain is due to the impact of the lossy nature of the supportive material at higher frequencies and it impacts more in the case of strip-based HHA.

Under 3-dB AR BW, the effect of supportive structure on beamwidth is investigated at 3 GHz, and results are shown in Fig. 9. For all cases, beamwidths maintain very close harmony between conductors only and with their supports.

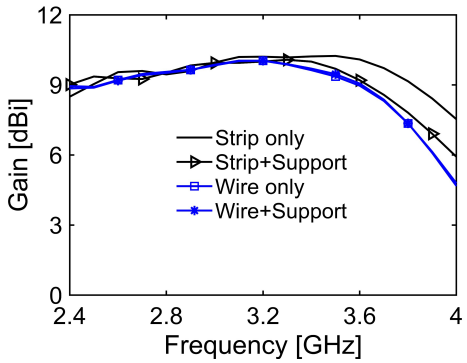

Figure 8. Impacts of support structure on gain.

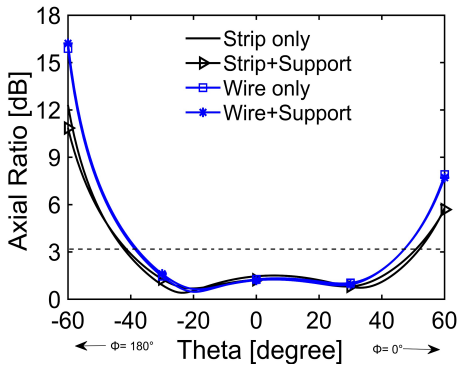

Figure 9. Impacts of support structure on 3-dB AR beamwidth.

4. FABRICATION AND EXPERIMENTAL RESULTS

As a first step of fabrication, a PLA material-based complete support structure is printed out using the 3-D printer (Sindoh 3D Wox). PLA filament of diameter 1.75 mm made by Overture is used as the only support material. The printer setting (nozzle and bed temperature) is maintained as per the description labeled on the spool of the filament. The structure is 100% filled with material, and it is also confirmed at the startup of the printing. To ensure successful printing, there is always a need for extra support which acts as a pillar for holding the intended spiral part and inclusively a part of the printing process. This extra unnecessary part is very thin and removed later to expose the original structure. Sandpaper and isopropyl alcohol are used for smoothing and cleaning the printed surfaces which facilitates the addition of conductive elements. As part of metallization, copper tape and ready-to-use conductive paints are used as two independent approaches. For the strip-based HHA, both conductive materials (copper tape and paint) are used in two different approaches. Copper tape in strip form is placed along the wide face of the flat spiral arm and on the square base of the 3-D printed structure. In another approach, instead of copper tape, silver-coated copper conductive paint is used on the wide face of the spiral arm (strip-based) and along the wire-like spiral arms (wire-based). The ground plane is also ensured by paint. Very fine paint brushes are used for painting the required conductive areas. The fabricated antennas are shown in Fig. 10. The cylindrical body of the SMA connector comes out through the pre-designed hole from the bottom of the square supportive base and is attached to the ground plane. The central core of the connector is fixed with the bottom end of the spiral strip or wire. To do so, direct soldering is used in the case of copper strip-based HHA. Instead of soldering, paint is used in the case of paint-based approaches.

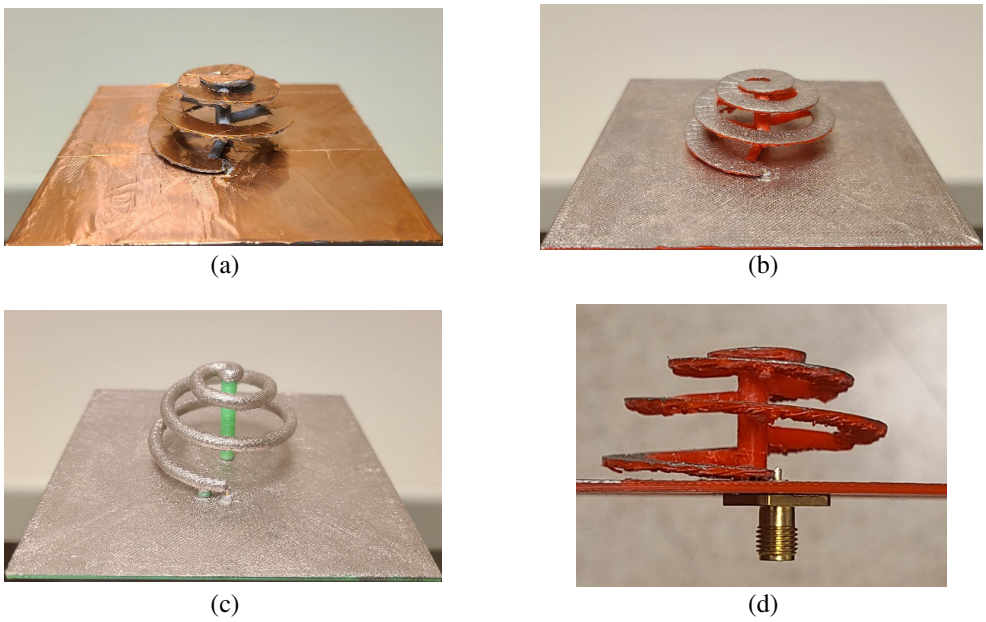

Figure 10. Fabricated antennas: (a) copper strip-based, (b) painted strip-based, (c) painted wire-based, (d) straight view with SMA connector.

To validate the numerical results, measurements are done using various equipment under a specific setup. The reflection coefficient (S_{11}) of the fabricated antennas is measured using an Agilent E8362C performance network analyzer. It is seen from Fig. 11 that the measured S_{11} for all the cases and approaches maintain $S_{11} \leq -10\,\text{dB}$ throughout the considered frequency range and agree with that of the simulation. It also confirms the matching of the input impedance of the hemispherical helical antenna without any extra impedance matching section. For both $\theta = 0^\circ$ and 30°, the 3-dB AR BW are very close for strip-based cases (copper strip and paint) except for the variation of AR values which

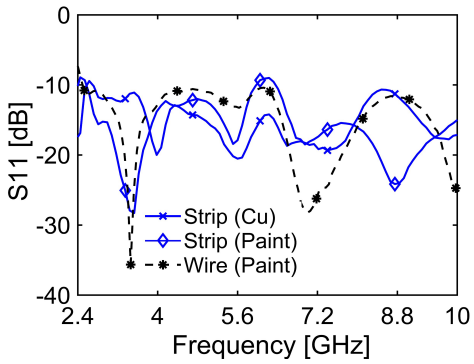

Figure 11. Measured reflection coefficients of HHA.

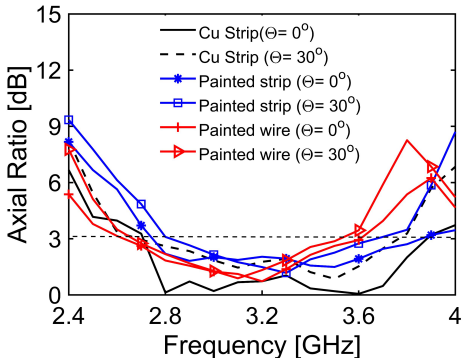

Figure 12. Measured axial ratios at boresight and away.

are shown in Fig. 12. At $\theta = 0°$, the copper strip-based HHA provides a maximum AR BW of 35% (2.72 GHz to 3.87 GHz) which is more than the BW [33% (2.75 GHz to 3.84 GHz)] of its paint-based counterpart. For wire-based HHA, the obtained percentage AR BW is 29.67% (2.67 GHz to 3.60 GHz). So, compared with numerical results (Fig. 7), a better %AR BWs is obtained for measured cases. The 3-dB AR BW for two different elevation angles is summarized in Table 1. Gain performances for all measured cases are in good agreement but performed poor compared to simulated results. There may be two reasons for this degradation of gain: the more lossy properties of the used PLA material at higher frequencies than the considered value in simulation, and the lower conductivity of the used copper tape and paint. It is seen from Fig. 13 that throughout the corresponding 3-dB AR BW, the measured gains for both strip and wire-based cases are 8 ± 1.35 dBi and 8.5 ± 0.75 dBi, respectively. The radiation patterns are measured in an anechoic chamber. The normalized far-field radiation at four different frequencies throughout the covered 3-dB AR bandwidths is shown in Figs. 14(a)–(d). All types (strip and wire) of HHA maintain similar radiation performances by maintaining the main beam in the axial direction ($\theta = 0°$) including symmetry. Beamwidths for all cases are measured at 3.3 GHz and shown in Fig. 15. The painted strip-based HHA outperforms other approaches. The total beamwidths of 98° and 118° are obtained from the copper and painted strip-based HHA, respectively. On the other hand, wire-based HHA provides a maximum beamwidth of 77°.

Table 1. The measured 3-dB AR BW at different elevation angles are summarized in Table 1.

Approaches	**3-dB AR BW**	
	$\boldsymbol{\theta = 0°}$	$\boldsymbol{\theta = 30°}$
Copper (Cu) strip	35% (2.72 GHz to 3.87 GHz)	32.05% (2.7 GHz to 3.73 GHz)
Painted strip	33% (2.75 GHz to 3.84 GHz)	27.10% (2.81 GHz to 3.69 GHz)
Painted wire	29.67% (2.67 GHz to 3.60 GHz)	27.70% (2.68 GHz to 3.54 GHz)

The difference between strip and wire-based helispherical antennas can be summarized in terms of performance parameters and fabrication issues and are mentioned as follows:

- For achieving self-matching of impedance, the wire-based approach requires more radiating surface area (wider circumference of the wire) than the width of the strip (strip-based approach).
- The strip-based approach provides better circular polarization bandwidth (3-dB AR BW) than its wire-based counterpart.
- In terms of gain, a wire-based hemispherical antenna performs better (improved gain with fewer variations throughout the band) than a strip-based approach.

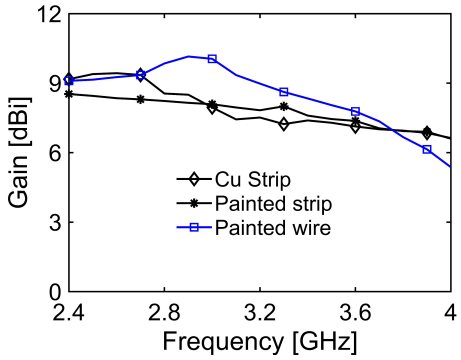

Figure 13. Measured gains among different approaches of HHA.

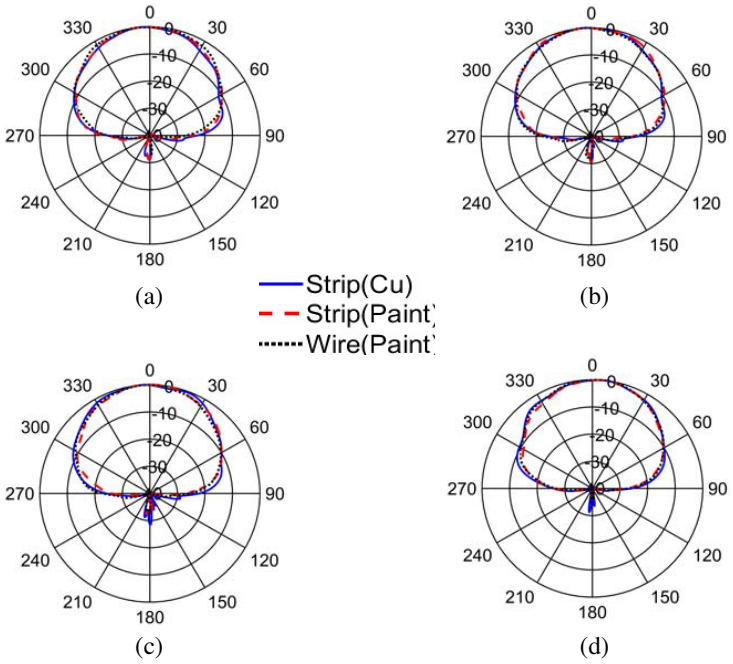

Figure 14. Normalized far field radiation patterns and beamwidths in XZ plane in the corresponding 3dB AR bandwidth ranges: (a) 3.0 GHz, (b) 3.2 GHz, (c) 3.4 GHz, (d) 3.6 GHz Polar and radial axes units were expressed in degree (°) and dB respectively.

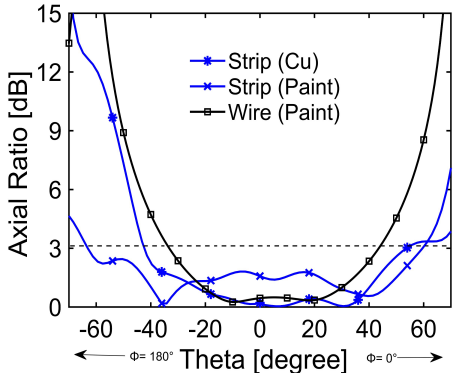

Figure 15. Minimum and maximum beamwidths.

- In the case of the strip-based case, circular polarization is obtained over a wider angular range (beamwidth) than in the wire-based case.
- For the wire-based case, no supportive branch was used for holding the spiral arm. If the wire diameter is increased too high then there is a chance of deformation of the wire due to gravity which may change the desired gap between turns and finally may degrade the antenna performance. Using additional supportive branches will solve the issue, but some areas of the spiral will remain non-conductive which may degrade the performance. On the other hand, there is no issue with using extra branches to hold the spiral for the case of the strip-based approach since the branches end at the bottom side (non-conductive area) of the flat spiral.

There is no mentionable difference in weight and fabrication costs between the wire and strip-based hemispherical helical antennas. Almost the same amount of printed materials (PLA-Polylactic acid) is needed for both approaches. Due to the bigger surface area of the wire-based spiral, it consumed almost twice the amount of conductive paint compared to the strip-paint-based case. But there is no significant cost variation between the conductive strip and the paint.

Overall, the performance parameter and the type of 3D-printed material for the proposed work are compared with some of the previously published articles and are shown in Table 2.

Table 2. Comparison with related works.

Ref. and Conductor Type	**Required extra section for impedance matching?**	**3-dB AR BW (%)**	**Gain (dBi)**	**Beamwidth (degrees)**	**Support Material**
[4] Wire	Yes	5	9.1	135	Polyethylene
[5] Wire	Yes	11	–	77	Not reported
[6] Wire	No	40	5.8	72	ABS + PETG
[13] Tapered strip	Yes	24	10	80	Balsa wood
[9] Strip	Yes	7	9	70	Polystyrene
This work	**No**	**35**	**9.35**	**118**	**PLA**

5. CONCLUSION

Additive manufacturing is successfully applied to the rapid prototyping of strip and thick wire-based hemispherical helical antennas. The broader width of the strip with non-conformal placement relative to the hemispherical surface and the wider diameter of the wire make the HHAs self-matched. Along with copper strip, conductive paint is used for the radiating part which provides a similar performance to the former one. The measured results agree well with the simulation. Including the mechanical stability, the HHA in this work can produce ultra-wideband impedance bandwidth without any extra matching section, a 3-dB axial ratio bandwidth of 35%, a maximum gain of 9.35 dBi, and a beamwidth of 118°. Due to the tighter geometry and smaller size, the proposed antenna has applications in aerospace, mobile communication, and INMARSAT satellite system. The 3D-printing technique broadened the design and construction flexibilities. By choosing the low-loss fabrication materials, work would be done in the future to improve the gain performance of the HHA.

REFERENCES

1. Al-Dulaimi, Z., T. A. Elwi, and D. C. Atilla, "Design of a meander line monopole antenna array based hilbert-shaped reject band structure for MIMO applications," *IETE Journal of Research*, Vol. 68, No. 1, 1–10, 2020.
2. Haleem, M. and T. A. Elwi, "Circularly polarized metamaterial patch antenna circuitry for modern applications," *Far East Journal of Electronics and Communications*, Vol. 26, 17–32, 2022.
3. Elwi, T. A., H. M. Al-Rizzo, Y. Al-Naiemy, and H. R. Khaleel, "Miniaturized microstrip antenna array with ultra mutual coupling reduction for wearable MIMO systems," *IEEE International Symposium on Antennas and Propagation (APSURSI)*, 2198–2201, Spokane, WA, 2011.
4. Elwi, T. A., "A miniaturized folded antenna array for MIMO applications," *Wireless Pers. Commun.*, Vol. 98, 1871–1883, 2018.
5. Al-Dulaimi, Z., T. A. Elwi, D. C. Atilla, and C. Aydin, "Design of fractal based monopole antenna array with ultra-mutual coupling reduction for MIMO applications," *18th Mediterranean Microwave Symposium (MMS)*, 39–42, Istanbul, 2018.
6. Ghadeer, S. H., S. K. Abd.Rahim, M. Alibakhshikenar, B. S. Virdee, T. A. Elwi, A. Iqbal, and M. A. Hasan, "An innovative fractal monopole MIMO antenna for modern 5G applications," *AEU — International Journal of Electronics and Communications*, Vol. 159, 154480, 2023.
7. Cardoso, J. C. and A. Safaai-Jazi, "Spherical helical antenna with circular polarization over wide beam," *Electron Lett.*, Vol. 29, 325–326, 1993.
8. Brister, J. A. and R. M. Edwards, "Design of a balanced ball antenna using a spherical helix wound over a full sphere," *Antennas & Propagation Conference*, 1–4, Loughborough, 2011.
9. Hui, H. T., K. Y. Chan, and E. K. N. Yung, "The low-profile hemispherical helical antenna with circular polarization radiation over a wide angular range," *IEEE Transactions on Antennas and Propagation*, Vol. 51, No. 6, 1415–1418, 2003.
10. Latef, T. A. and S. K. Khamas, "Measurements and analysis of a helical antenna printed on a layered dielectric hemisphere," *IEEE Transactions on Antennas and Propagation*, Vol. 59, 4831–4835, 2011.
11. Chen, C. H., B. J. Hu, Z. H. Wu, and E. K. N. Yung, "A self-matching hemispherical helical antenna," *IEEE Antennas and Propagation Society International Symposium*, 4709–4712, 2006.
12. Yan, Y., Q. Nan, C. Liu, Y. Zhang, and J. Li, "3D-printed hemispherical helix GPS antenna with stable phase center," *International Applied Computational Electromagnetics Society Symposium*, 1–2, China, 2019.
13. Alsawaha, H. W. and A. Safaai-Jazzi, "Ultrawideband hemispherical helical antennas," *IEEE Transactions on Antennas and Propagation*, Vol. 58, No. 10, 3175–3185, 2010.
14. Yang, H.-M., Y.-G. Zhou, H.-Z. Wang, H.-Z. Jiang, and Y.-C. Chen, "An ultra-wideband circularly polarized hemispherical helical antenna," *IEEE 4th International Conference on Electronic Information and Communication Technology (ICEICT)*, 222–226, 2021.
15. Zhang, Y. and H. T. Hui, "A printed hemispherical helical antenna for GPS receivers," *IEEE Microwave and Wireless Components Letters*, Vol. 15, 10–12, 2005.
16. Kim, O. S., "Rapid prototyping of electrically small spherical wire antennas," *IEEE Transactions on Antennas and Propagation*, Vol. 62, 3839–3842, 2014.
17. Ghosh, P. and F. Harackiewicz, "3D printed low profile strip-based helical antenna," *Progress In Electromagnetics Research C*, Vol. 127, 195–205, 2022.
18. Ghosh, P. and F. J. Harackiewicz, "Three-dimensional-printed strip and paint-based semiellipsoidal helical antenna," *Microwave and Optical Technology Letters*, Vol. 65, No. 8, 2262–2266, 2023.
19. Mei, J. N., D. W. Ding, and G. Wang, "Design of compact wideband circularly polarized conical helix," *International Conference on Computer Information Systems and Industrial Applications*, 139–141, 2015.

20. Ernest, A. J., Y. Tawk, J. Constantine, and C. G. Christodoulou, "A bottom fed deployable conical log spiral antenna design for CubeSat," *IEEE Transactions on Antennas and Propagation*, Vol. 63, No. 1, 41–47, 2015.
21. Tang, X., Y. He, and B. Feng, "Design of a wideband circularly polarized strip helical antenna with parasitic patch," *IEEE Access*, Vol. 4, 7728–7735, 2016.
22. Tang, X., B. Feng, and Y. Long, "The analysis of a wideband strip helical antenna with 1.1 turns," *International Journal of Antennas and Propagation*, Vol. 2016, No. Article ID 5950472, 2016.
23. Helena, D., A. Ramos, T. Varum, and J. N. Matos, "Antenna design using modern additive manufacturing technology: A review," *IEEE Access*, Vol. 8, 177064–177083, 2020.